

# Effect of Gravity on the Nonlinear Dynamics of an Overhung Rotor with Annular Rubs

Elijah Chipato\*, A D Shaw\* and M I Friswell\*

\*College of Engineering, Swansea University Bay Campus, Fabian Way, Crymlyn Burrows, Swansea SA1 8EN, UK

*Summary.* In this study a mechanical model of an overhung rotor is explored to determine the effect of gravity on the nonlinear dynamics of an aero-engine. The model is an overhung disc with rotor-stator contact; the model has two degrees of freedom with lumped parameters, friction is neglected in the contact and the equations of motion are non-dimensionalised. A parametric study of the non-dimensional gravity parameter  $\hat{g}$  is conducted. The bifurcation plots show that gravity plays a crucial role in the non-linear dynamics of such systems. With zero gravity, as explored in earlier studies, the model has periodic synchronous solutions in the stationary frame, and periodic solutions in the rotating frame produced an internal resonance that appear non-periodic in the stationary frame. If the gravity parameter is non-zero, then the dynamics observed are much richer and show additional period-2, period-3, period-7 and chaotic solutions in the stationary frame and continuous contact (full annular rub).

## Introduction

Rotor stator contact affects many rotating machines from drill strings to aero-engines. In most cases the rub is initiated by static unbalance. There are three major classes of rotating machinery vibrations namely axial, torsional and lateral vibration. For aero engines lateral vibrations are the most destructive type of vibration and can include forward, backward and chaotic whirls. Forward whirl is synchronous and the rotor orbits in the same direction as the rotor spin, whereas backward whirl is more destructive and characterized by an orbiting rotor opposite to the direction of rotor spin and is initiated by the presence of a large frictional force. In chaotic whirl there is no preferential orbit of the rotor and it bounces in any direction. Whirling shafts or rotors can subsequently interact with the stator/enclosure. This rubbing action can also change the nature of the whirl. Ehrich [1] gave a comprehensive study of a number of rubbing phenomenon observed in turbo-machinery, including period doubling, chaos and subharmonic resonances. Some of these phenomenon were also observed in the present study, namely period doubling and chaos. Vijayan et al. [2] studied the influence of rotor rub on backward whirl of a two disk rotor and found that vibration modes excited in the system can be changed by altering the phase differences between eccentric masses of the two disks and suggested that this controlled the initiation of backward whirl since altering the eccentric masses might initiate continuous rubbing which increases the friction in the system. Shaw et al. [3] suggested that bouncing periodic motion can be initiated by an internal resonance condition in the system and stressed that this internal resonance condition is only considered as a necessary rather than sufficient condition for the onset of this motion; this motion was termed asynchronous partial contact orbits.

In other work, Zhou et al. [4] studied a nonlinear model of a rotor seal system including the coupled effects of gravity, Muszynska's nonlinear seal fluid dynamic force and mass eccentricity. This system is analysed using bifurcation diagrams, time history plots, orbit plots, Poincaré maps and spectra and as the rotational speed is increased rich forms of dynamic behaviour were found including periodic, multi-periodic, quasi periodic and chaotic dynamic motion. The effects of seal drop pressure, seal length, seal clearance, distance between the two disks and mass of the discs on the dynamics of the system was investigated and it was found that high seal drop pressure, an optimised seal clearance, long seal length and a symmetrical disc structure can enhance the stability of a double disc rotor-seal system.

Hui et al. [5] performed a comprehensive study of oil film instability in an overhung rotor system with flexible coupling misalignment. A finite element model of the overhung rotor system with gyroscopic effects was used and sliding bearings were simulated using a nonlinear oil film force model using the assumption of short-length bearings. The FE model was validated using experimental data. Their study shows that under perfectly aligned conditions, the onset of first and second vibration mode instability in a run down are less than during run up due to the hysteresis effect, this can also be viewed as the presence of multiple solutions, with different initial conditions finding different solutions. When misaligned there was a delay in the onset of the first vibration mode instability and this resulted in a decrease in the vibration amplitude.

Yang et al. [9] used time-frequency techniques for rub-impact detection in rotating machinery. The authors introduced a new method based on the fast oscillation characteristics of instantaneous frequency to detect rub-impact faults of rotor bearing systems. A fast time varying transient stiffness(stiffening effect) of rub impact was formulated and a time frequency technique called the nonlinear squeezing time frequency transform was introduced to extract the instantaneous frequency. They show that the instantaneous frequency of the vibration response remained constant at the rotor spin speed if there is no rub-impact fault. However, the instantaneous frequency oscillated periodically around the basic harmonic frequency (rotor spin frequency) whenever a rub impact fault occurred. Their proposed new analysis method was also validated using experiments.

Wang et al. [10] investigated the sudden unbalance and rub-impact caused by a blade off scenario in an overhung rotor and used both theoretical and experimental approaches to study the system. Their results reveal that the sudden unbalance caused by blade loss will introduce an impact effect in the rotor and the frequency spectrum shows that the first critical speed frequency (including the backward whirling frequency) exists in the frequency content except for the rotational speed frequency peak. Also, the authors noted that rubbing action between the rotor and constraint ring induces a load path to absorb the unbalance loads and generates additional stiffness which causes the resonance speed to rise and the



' ) represents a nondimensional quantity and a derivative with respect to nondimensional time respectively

$$\begin{cases} \phi_y'' - \hat{J}_p \theta' \phi_x' + 2\zeta \phi_y' + \hat{\phi}_y = \hat{m} \hat{e} (\theta'^2 \cos \theta + \theta'' \sin \theta) + \hat{M}_{\phi_y} \\ \phi_x'' + \hat{J}_p \theta' \phi_y' + 2\zeta \phi_x' + \hat{\phi}_x = \hat{m} \hat{e} (\theta'' \sin \theta - \theta'^2 \cos \theta) + \hat{M}_{\phi_x} + \hat{m} \hat{g} \\ \hat{M}_{\phi_y} = H(\|\hat{r}_c\| - 1) \beta \hat{\phi}_y \left( \frac{1}{\sqrt{\phi_x^2 + \phi_y^2}} - 1 \right) \\ \hat{M}_{\phi_x} = H(\|\hat{r}_c\| - 1) \beta \hat{\phi}_x \left( \frac{1}{\sqrt{\phi_x^2 + \phi_y^2}} - 1 \right) \end{cases} \quad (4)$$

where  $\hat{g} = \left( \frac{g}{c^* \omega_n^2} \right)$ ,  $\beta$  is the ratio between snubbing stiffness and the linear stiffness of the rotor  $\left( \frac{k_s}{k_r} \right)$  and  $k_r = \left( \frac{k_\phi}{b^2} \right)$ ;

## Numerical analysis and results

The numerical analysis in this study used the fourth order Runge-Kutta numerical method with an adaptive step control to lower the local truncation error at every step. Representative test parameters are shown in Table 1 following the studies made by Zilli et al. [23]. The numerical calculation made use of the ODE45 solver in MATLAB and the events function was used to identify the exact point where contact is made which will trigger the step control mechanism to reduce the step size for accuracy during contact. To perform numerical calculations on the system, Equations (4) can be transformed into

**Table 1: Nondimensionalised system parameters**

Symbol	Parameter	Value
$\hat{m}$	Normalised mass	0.9285
$\hat{J}_p$	Normalised polar moment of inertia	0.143
$\beta$	Stiffness nonlinearity	1.32
$\hat{e}$	Normalised rotor eccentricity	0.494
$\zeta$	Damping ratio	0.01

the form

$$\mathbf{M}\ddot{\mathbf{q}} + \Omega \mathbf{G}\dot{\mathbf{q}} + \mathbf{K}\mathbf{q} + \mathbf{D}\dot{\mathbf{q}} = \mathbf{N}(\mathbf{q}, \dot{\mathbf{q}}) \quad (5)$$

where  $\mathbf{M}$ ,  $\mathbf{G}$ ,  $\mathbf{C}$ ,  $\mathbf{K}$ , are the mass, gyroscopic, damping and stiffness matrices of the system,  $\mathbf{N}(\mathbf{q}, \dot{\mathbf{q}})$  is the nonlinear matrix representing rotor stator contact. To perform numerical calculations it is convenient to transform Equation (5) into state space form.

### Bifurcation Analysis

Bifurcation diagrams show the qualitative changes that occur as a system parameter is varied; in rotordynamics, rotor spin speed is one of the main control parameters which is varied. In this study both the gravity parameter,  $\hat{g}$  and the dimensionless rotor spin speed are used as control parameters. Figure 2 shows bifurcation diagrams where  $\hat{g}$  is varied for two different rotor spin speeds which lie inside and outside the bistability zone for the zero gravity case studied by [23] shown in Figure 3a. This enables the values of  $\hat{g}$  with interesting solutions to be studied. Figure 2 shows that for high values of  $\hat{g}$  the rotor remains in contact with the stator (full annular rub) and that static displacements dominate the response. From Figure 2 values of  $\hat{g}$  of 0, 1.27, 2 and 3.44 were chosen for further study. It is important to note that the zero gravity case,  $\hat{g} = 0$  was studied in [23]. Figure 3 shows the bifurcation analysis for the effect of rotational speed,  $\hat{\Omega}$ , on the dynamics of the overhung rotor system for different values of  $\hat{g}$ .

Bifurcation diagrams might appear to show chaos in many cases but often these cases turnout to be quasi-periodic/ asynchronous rather than truly chaotic. Therefore, to characterize the dynamics of the system more conclusively, particularly for chaos, the largest Lyapunov exponent spectra for the four cases are computed [26, 28] and shown in Figure 4. The largest Lyapunov exponents gives a direct measure of sensitive dependence on initial conditions (SDIC) [24–26]. A positive largest Lyapunov exponent shows that there is chaotic motion on a strange attractor. If the largest Lyapunov exponent is zero then we have periodic/ quasi-periodic motion and if the largest Lyapunov exponent is negative then the stable critical point is an attractor [27]. From Figure 4a, which is the zero gravity case, it is observed that the Lyapunov exponents of the system are negative for all values of  $\hat{\Omega}$  with the exception of  $\hat{\Omega} = 2$  where the Lyapunov exponent approaches zero and no chaotic vibrations are detected at this point.

However, increasing the gravity parameter to 1.27 and 2 will result in richer dynamics of the system being observed and now include chaos, period doubling and period 7 motions. As the gravity parameter was further increased to 3.44, it was noted that no chaos was detected although the dynamics are still richer than the zero gravity case with period doubling and period-7 motions. In this case the static deflection due to gravity dominates the response and full annular rub is often experienced. However the rotor still has solutions where it bounces in and out of contact. Figure 5 shows the vibration responses, orbit trajectories, Poincaré maps and amplitude spectra in both the stationary and rotating frames. Figure 5b

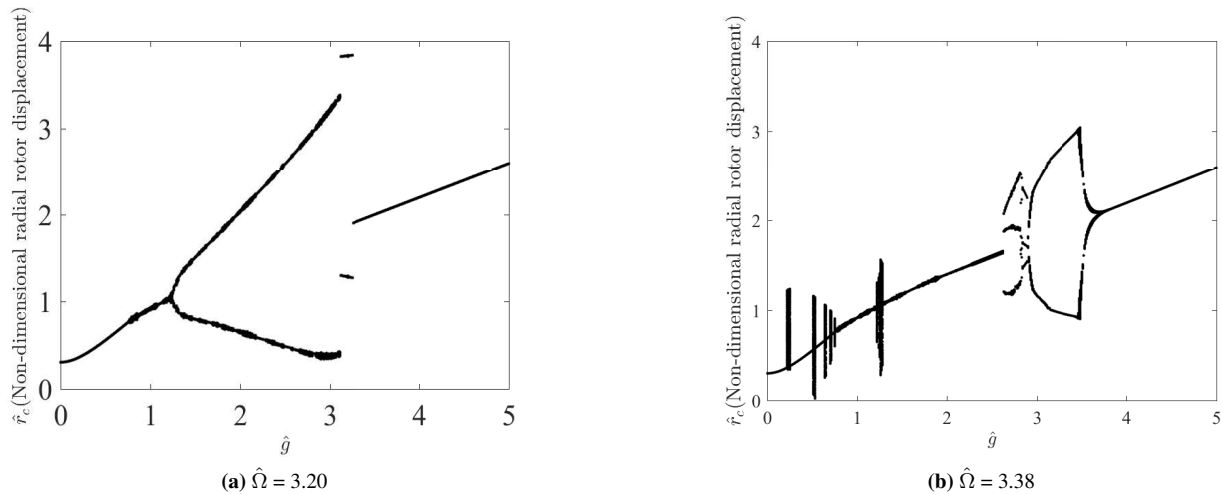


Figure 2: The bifurcation plots with  $\hat{g}$  for two rotor spin speeds

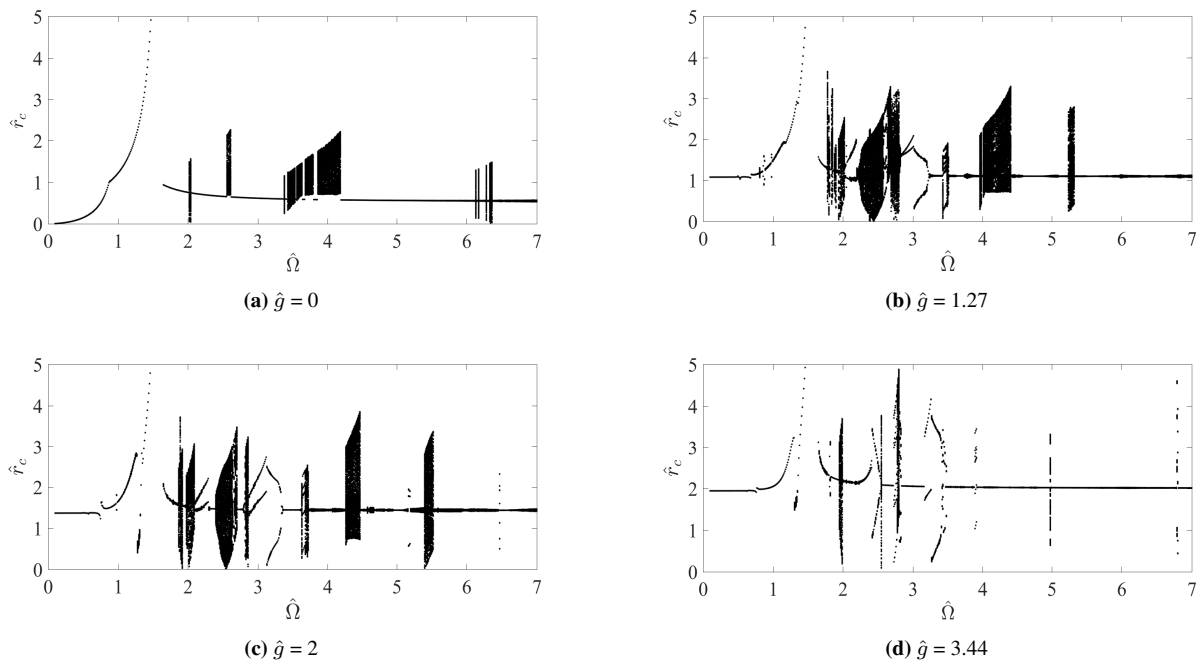


Figure 3: The bifurcation plots with rotor spin speed for different values of  $\hat{g}$ .

shows that the motion is not periodic when viewed in the stationary frame as the orbit shows that the rotor is in continuous precession. However, viewing the motion in the rotating frame shows that the motion is rather simple and periodic [3]. To better understand the response an FFT of the lateral displacement,  $\phi_x$ , in both stationary and rotating frames is taken. In the stationary frame three peaks are observed at 3.46, 1.319 and 0.856. The first frequency corresponds to the rotor spin speed/ excitation frequency, the other two frequencies correspond to the first forward and backward whirling frequencies as shown in the Campbell diagram in Figure 6. The value of the forward and backward whirling frequencies at a reference speed of 3.47 is found to be 1.2784 and 0.7822 and are slightly lower than the values obtained from the FFT by 3% and 9% respectively. Since the frequencies obtained from the Campbell diagram are lower than that of the FFT this can be regarded as a stiffening effect induced by the stator. However, something more interesting happens in the rotating frame, the peaks obtained from Figure 5h are 2.151 and 4.326 and these two frequencies are in a 2:1 ratio. The FFT for rotating frame only shows two peaks, unlike that of stationary frame which has three peaks, because in the rotating frame the unbalance force is not harmonic but static and therefore the third peak in the FFT for stationary frame which represents the rotor spin frequency does not appear in the FFT for rotating frame. The whirl velocities in the stationary frame can be related to that of the rotating frame as shown by equation (6) [3],

$$\hat{w}_r = \hat{w}_s + \hat{\Omega} \quad (6)$$

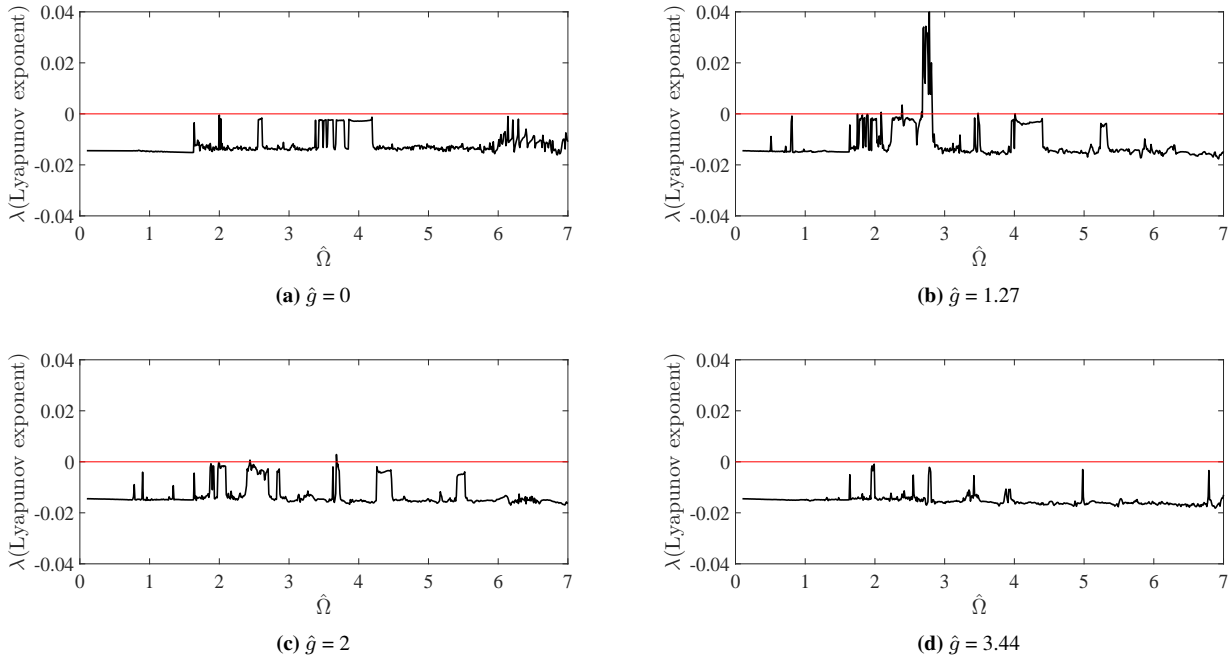


Figure 4: The largest Lyapunov spectra for different values of  $\hat{g}$ .

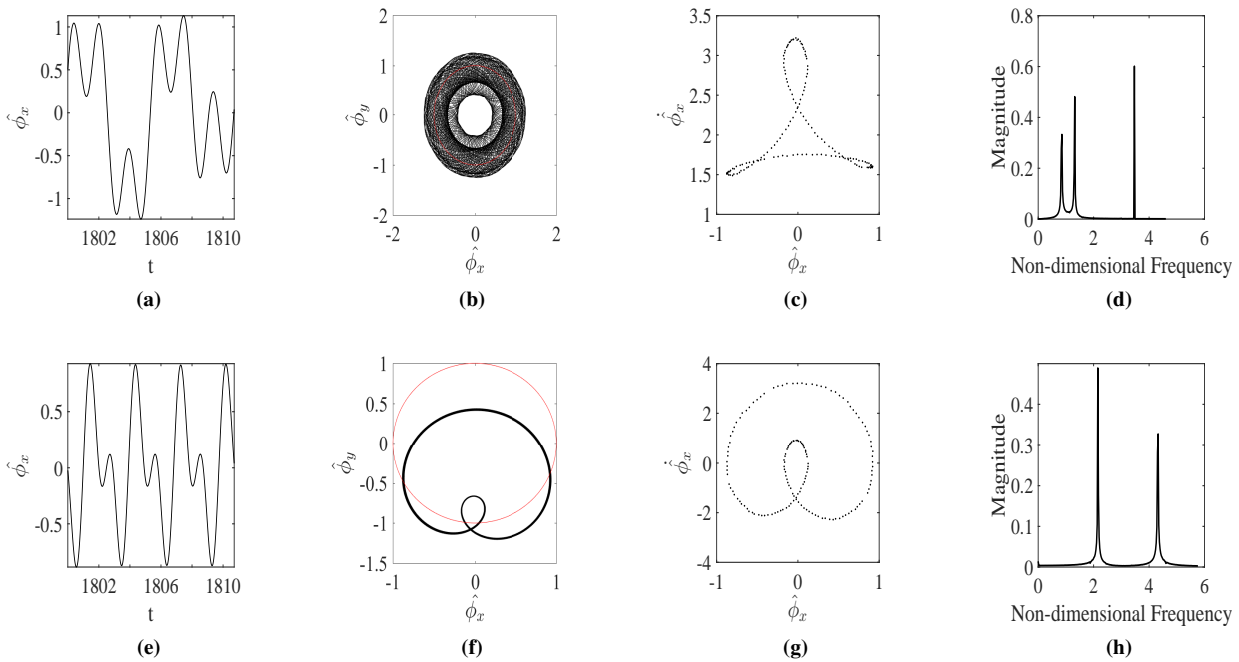


Figure 5: Vibration responses (5a and 5e), phase trajectories (5b and 5f), Poincaré maps (5c and 5g) and amplitude spectra (5d and 5h) for  $\hat{\Omega} = 3.47$  for the zero gravity case,  $\hat{g} = 0$ . Figures (5a - 5d) are for stationary frame and figures (5e - 5h) are for the rotating frame of reference.

where  $\hat{w}_r$  is the whirling speed in rotating frame and  $\hat{w}_s$  is the whirling speed in stationary frame. This therefore shows that to convert the frequencies obtained from the FFT for the rotating frame one should subtract the rotor spin speed. This then gives  $0.856 = (4.326 - 3.47)$  and  $-1.319 = (2.151 - 3.47)$  which corresponds to the values obtained from the FFT of the stationary frame. The fact that both the forward and backward whirling frequencies are present in both frames is an interaction/ energy exchange taking place between the FW mode and BW mode that is to say an internal resonance. Figure 4b shows the largest Lyapunov spectrum for  $\hat{g} = 1.27$  and shows that gravity introduces some chaos into the system since at rotor spin speeds 2.09, 2.39 and 2.68 to 2.82 the largest Lyapunov exponents are positive.

Figure 7 shows period-7 motion and Figure 8 chaotic motion for  $\hat{g} = 1.27$  for both stationary and rotating frames. It was noted that the character of the dynamics is the same in both frames, that is, the simplification in the rotating frame (see Figure 5) for  $\hat{g} = 0$  does not happen for  $\hat{g} = 1.27$ . Figure 8a - 8d shows the results for  $\hat{\Omega} = 2.61$  for stationary frame. The

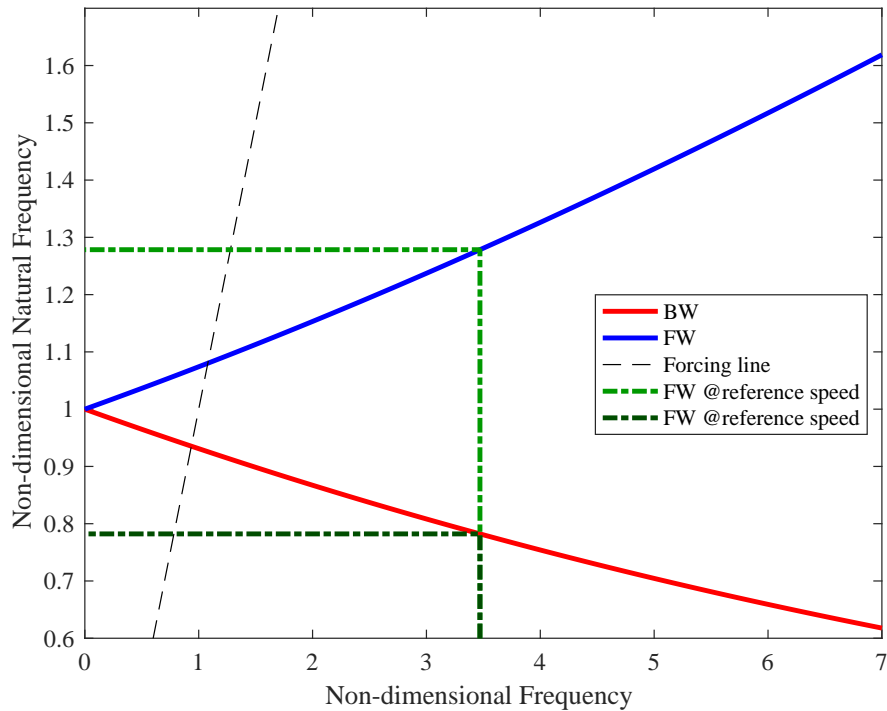


Figure 6: Campbell diagram showing forward and backward whirl speed at reference rotor spin speed  $\hat{\Omega} = 3.47$

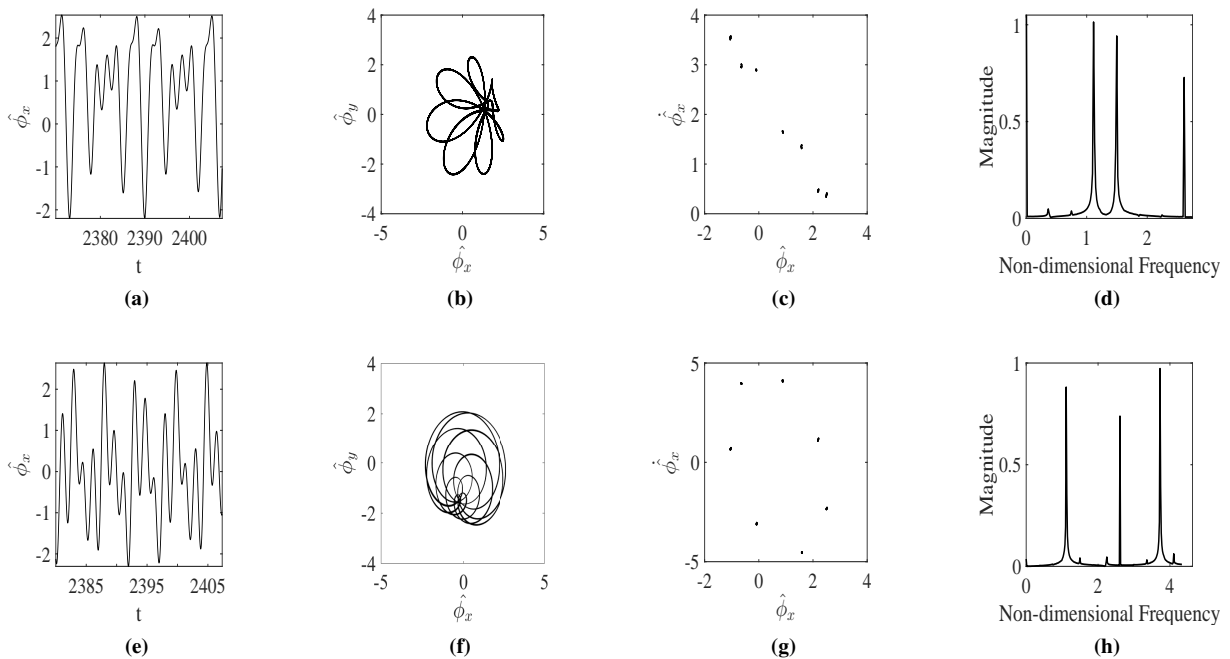
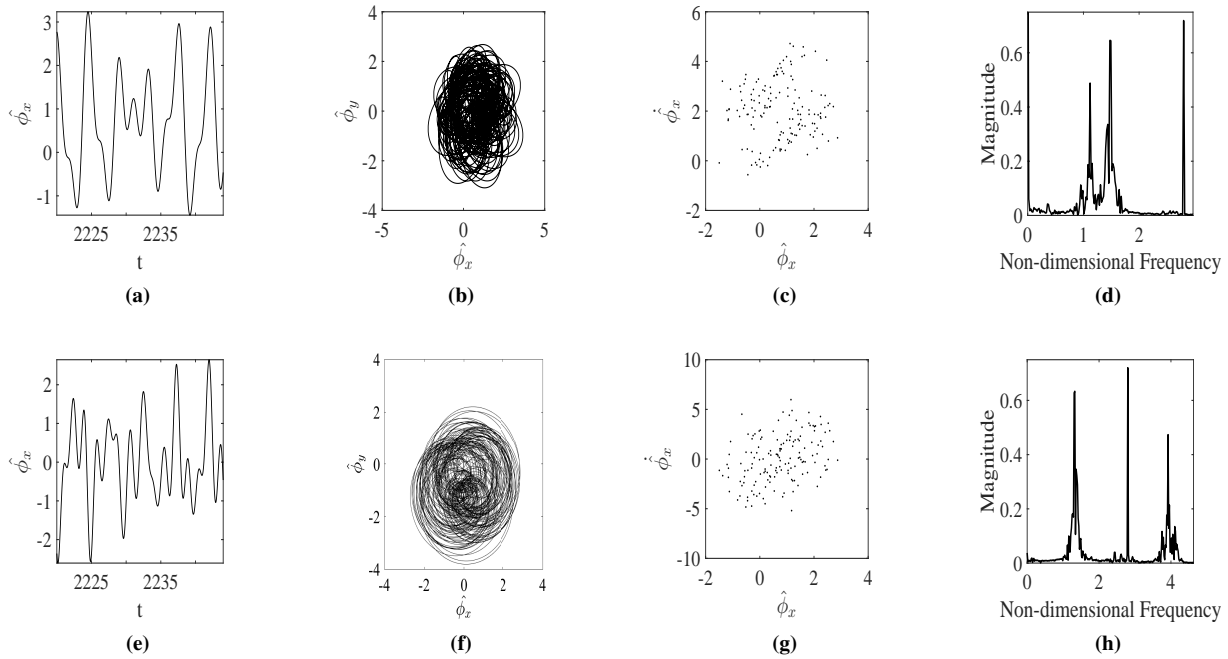


Figure 7: Vibration responses (7a and 7e), phase trajectories (7b and 7f), Poincaré maps (7c and 7g) and amplitude spectra (7d and 7h) for  $\hat{\Omega} = 2.61$  for  $\hat{g} = 1.27$ . Figures (7a - 7d) are for stationary frame and figures (7e - 7h) are for the rotating frame of reference.

Poincaré map shown in Figure 8c shows that the motion is period -7, the FFT in figure 8d shows 3 peaks at 1.114, 1.1496 and 2.61. The last peak is the excitation frequency (rotor spin speed) and the other two seem are related to the BW and FW at a reference speed of 2.61 but with a more significant difference than in the zero gravity case. The reason of this huge difference could be that increasing the gravity parameter will mean that there is more significant contact and therefore more stiffening which results in the significant difference between the Campbell diagram values and FFT frequency values. Also note that the FFT for the rotating frame now has 3 peaks unlike for the zero gravity case where it only had two. The reason for this observation is that in the rotating frame although the unbalance force is static, gravity is



**Figure 8: Vibration responses (8a and 8e), phase trajectories (8b and 8f), Poincaré maps (8c and 8g) and amplitude spectra (8h and 8d) for  $\hat{\Omega} = 2.80$  for  $\hat{g} = 1.27$ . Figures (8a - 8d) are for stationary frame and Figures (8e - 8h) are for the rotating frame of reference.**

harmonic and therefore the rotor spin frequency peak appears. Figures (8e - 8h) shows the response, orbit, Poincaré map and FFTs obtained for a rotor spin frequency of 2.80 for both stationary and rotating frames. The plots show evidence of chaos as the orbits show strange attractors, the Poincaré maps have points which are distributed in no particular order and the FFTs show a broadband response showing the presence of finite frequency components in the time series signal.

## Conclusions

In this paper the effect of gravity on the nonlinear vibration phenomenon of an overhung rotor was investigated. The 4th order Runge Kutta method was used to obtain bifurcation diagrams, Lyapunov exponent spectra, amplitude spectra, orbit diagrams, phase trajectories and Poincaré maps that show the nonlinear behaviour of the rotor system. After nondimensionalising the equations of motion it was noted that the gravity parameter is a function of shaft stiffness. It was noted that when the shaft stiffness of the rotor is high, the gravity parameter is very small. This is the case explored earlier studies and can be safely approximated to a zero gravity term. However, the opposite case of low shaft stiffness was explored in this study. The results presented here show that gravity introduces rich dynamic phenomenon into the rotor. For the zero gravity case the system only had periodic and quasi periodic solutions. Upon increasing the gravity parameter the system now exhibited period-2, period-7 and chaotic solutions. It was also observed that visualising the dynamic motion of systems in the rotating frame can give more insight into the nature of the solutions particularly for the zero gravity case. However, while there are situations where transforming to the rotating frame shows a periodic response to some thing that is aperiodic in the stationary frame, the opposite is never true - an aperiodic orbit in the rotating frame never becomes periodic on translation to the stationary frame.

## References

- [1] Ehrich F.F (1977) Observations of non-linear phenomena in rotordynamics. *Journal of System Design and Dynamics*,**2**,641.
- [2] Vijayan K., Vljajic N., Friswell M. I (2014), The Influence of Drillstring-Borehole Interaction on Backward Whirl. International Conference on Noise and Vibration Engineering, ISMA
- [3] Shaw A.D., Champneys A.R., Friswell M.I. (2016) Asynchronous partial contact motion due to internal resonance in multiple degree-of-freedom rotordynamics. *Proc. R.Soc A* 472: 20160303
- [4] Zhou W., Wei X., Wei X., Wang L. 2014. Numerical analysis of a nonlinear double disc rotor-seal system. *Journal of Zhejiang University SCIENCE A (Applied Physics and Engineering)*, **15**(1):39-52. [doi: 10.1631/jzus.A1300230]
- [5] Hui M., Xueling W., Heqiang N., Bangchun W. 2015. Oil-film instability simulation in an overhung rotor system with flexible coupling misalignment." *Archive of Applied Mechanics*, **85**(7):893-907. [doi:10.1007/s00419-015-0998-3]
- [6] Muszynska. A. 2005. *Rotordynamics*(CRC Press, Taylor and Francis, Boca Raton, FL)
- [7] Edwards S., Lees A. W., Friswell M. I (1999) The influence of torsion on rotor/stator contact in rotating machinery. *Journal of Sound and Vibration*, **225**(4):767-778
- [8] Ren Z. H., Yu T., Luo Y. G., Song N. H., Wen B. C (2007) Research on Rubbing Fault in a Dual-Disc Overhung Rotor-Bearing System. *Key Engineering Materials* **353**: 977-98.
- [9] Yang L., Chen X., Wang S., Zuo H. Rub-Impact Detection of Rotor Systems Using Time-Frequency Techniques. ASME. ASME International Mechanical Engineering Congress and Exposition, Volume 4B: Dynamics, Vibration, and Control [ doi:10.1115/IMECE2016-65412].
- [10] Wang C, Zhang D, Ma Y., Liang Z., Hong J (2016) Theoretical and experimental investigation on the sudden unbalance and rub impact in rotor system caused by blade off, *Mechanical Systems and Signal Processing*, **76**:111-135
- [11] Muszynska, A., 1989, "Rotor-To-Stationary Element Rub-Related Vibration Phenomena in Rotating Machinery—Literature Survey," *The Shock and Vibration Digest*, **21**(3):3-11.
- [12] Jun, J., and Yanhua, C (2013) Advances in the Research on Nonlinear Phenomena in Rotor/Stator Rubbing Systems *Chinese Journal of Advances in Mechanics* **43**(1): 132-148
- [13] Muszynska A., Bently D. E., Franklin W.D., Hayashida R. D., Kingsley L. M., Curry A. E (1989) Influence of rubbing on rotordynamics-Part1, "Nasa Report-Bently Rotordynamics research corporation"
- [14] Muszynska A., Bently D. E., Franklin W.D., Hayashida R. D., Kingsley L. M., Curry A. E (1989) Influence of rubbing on rotordynamics-Part2, "Nasa Report-Bently Rotordynamics research corporation"
- [15] Ehrich, F. F (1988) High Order Subharmonic Response of High Speed Rotors in Bearing Clearance. *Journal of Vibration and Acoustics*. **110**(1): 9-16.
- [16] Muszynska A., Franklin W. D., Hayashida R. D (1991) Rotor-to-stator partial rubbing and its effects on rotor dynamic response.
- [17] Chu F., Lu, W (2005) Experimental observation of nonlinear vibrations in a rub-impact rotor system. *Journal of Sound and Vibration* **283**, :621-643.
- [18] Hou L., Chen Y., Cao Q (2014) Nonlinear vibration phenomenon of an aircraft rub-impact rotor system due to hovering flight. *Communications in Nonlinear Science and Numerical Simulation*. **19**(1):286-297.
- [19] Lahriri S., Weber H.I., Santos I. F., Hartmann H (2012) Rotor stator contact dynamics using a non-ideal drive Theoretical and experimental aspects *Journal of Sound and Vibration* **331**(20):4518-4536
- [20] Junyi C., Chengbin M., Zhuangde J., Shuguang L (2011) Nonlinear dynamic analysis of fractional order rub-impact rotor system .*Communications in Nonlinear Science and Numerical Simulation* **16**(3):1443-1463
- [21] Khanlo H.M., Ghayour M., Ziaei-Rad S (2011) Chaotic vibration analysis of rotating, flexible, continuous shaft-disk system with a rub-impact between the disk and the stator. *Communications in Nonlinear Science and Numerical Simulation* **16**(1):566-582
- [22] Jang-Der J., Lu H., Chien-Wan H., Chung-Yi C (2014) Identification for Bifurcation and Responses of Rub-impacting Rotor System. *Procedia Engineering* **79**:369-377
- [23] Zilli A., Williams R.J., Ewins D.J (2015) Non-linear dynamics of a simplified model of an overhung rotor subjected to intermittent annular rubs. *Journal of Engineering Gas Turbines and Power* **137**(6)
- [24] Strogatz S. H (1994) *Nonlinear Dynamics and Chaos: With Applications to Physics, Biology, Chemistry, and Engineering*. New York: Addison-Wesley.
- [25] Nayfeh A.H., Balachandran B (1995) *Applied Nonlinear Dynamics: Analytical, Computational, and Experimental Methods*. New York: John Wiley and Sons.
- [26] Wolf A., Swift J.B., Swinney H. L., Vastano J. A (1985) Determining Lyapunov exponents from a time series. *Physica Nonlinear Phenomena* **16**(3):285-317.
- [27] Moon F (2004) *Chaotic vibrations : an introduction for applied scientists and engineers*. New York. Chichester : Wiley
- [28] Thomsen., J.J (1997). *Vibrations and Stability: Order and Chaos* (McGraw-Hill, Maidenhead).